Cross-Band Interaction Mitigation in Dual-Band Antenna Arrays for 4G/5G and Beyond

Yingjian Xiong[1], Can Ding[2], Zhiqun Cheng[1], Y. Jay Guo[2]
[1] (Affiliation): School of Electronics and Information Engineering, Hangzhou Dianzi University, Hangzhou, China, yingjian_xiong@qq.com
[2] (Affiliation): Global Big Data Technologies Centre (GBDTC), University of Technology Sydney (UTS), Sydney, Australia, can.ding@uts.edu.au

***Abstract*—Collocating antennas for different purposes on a single communication platform is a big trend as it can improve space efficiency. However, strong interferences happen among the antennas working at different bands due to the close proximity, leading to deteriorated antenna performance. This paper proposes a simple yet effective method to alleviate this issue by developing low-scattering array topology without increasing array size. The proposed method is used on a typical 3G/4G dual-band dual-polarized base station antenna array as an example to illustrate its effectiveness. By relocating the positions of the antennas in such array, the antenna performance can be substantially enhanced. Although this technique cannot eliminate the interferences solely, it can be used as a supplementary with other techniques to achieve optimal performance. At last, the proposed array topology is used together with a low-scattering spiral antenna designed for cross-band scattering mitigation, which leads to an outstanding array performance with a compact size.**

***Index Terms*—Array topology, base station antenna, cross-band interaction, decoupling, spiral low-scattering antenna.**

I. INTRODUCTION

The fifth-generation (5G) mobile communication systems are widely regarded as a cornerstone of the fourth industrial revolution. Although 5G standardization activities have rightly focused on the definition of the air-interface and network protocols, it is now becoming imperative for the mobile industry as a whole to develop the new antenna technologies that will address the challenges in deploying 5G base stations and networks.

Base station antenna (BSA) technologies will play a crucial role in determining the performance and the deployment cost of 5G. Owing to the rapidly rising costs and environmental pressures when operators are acquiring new sites for their base station antennas, one of its panels normally accommodates several antennas working in different frequency bands and with different polarizations. For instance, each panel covering one sector in currently deployed 3G/4G base station antenna arrays hosts two kinds of arrays in a side-by-side configuration within one cover (radome) [1]. Strong interferences occur among the closely spaced antenna elements. In particular, the low band (LB) antenna elements with larger size act as big scatterers and impose significant negative effects on the high band (HB) antenna elements, deteriorating both of their S parameters and radiation patterns. This cross-band interference problem is critical and will be more severe when 5G antenna elements are added on the base station platform.

To mitigate the LB antennas' interferences on HB antenna elements in a compact dual-band or multi-band antenna array, several types of solutions were proposed. The traditional solution is to utilize different kinds of metal baffles or walls [2-3]. By optimizing the sizes and positions of the parasitic elements, the performance can be enhanced to some extent. The second solution is mantle cloaking techniques based on scattering cancellation [4-6]. By covering the LB antenna element with patterned metasurfaces, the HB radiation reflected by the LB element and the metasurface can be cancelled, thus the LB antenna can be made "invisible" to the HB radiation at certain frequencies. The third kind of solution is based on choking techniques or filtering antennas [7-9]. This is realized by redesigning the LB radiator to make it have the low-pass high-stop filtering characteristic. In this way, the HB radiation will induce minimum currents on the LB radiator, thereby the LB element has little negative effect on the HB element. All the aforementioned techniques are effective but the working bandwidth is limited. The available methods can only suppress the LB elements' interferences on the HB radiation within a limited bandwidth. For example, in [7], by choking the LB element, the HB performance is recovered within the band from 1.7 to 2.3 GHz. However, a typical 4G base station application require the HB antenna to cover a wider bandwidth from 1.7 to 2.7 GHz. Entering the 5G era, some BSAs can also cover the 5G sub-6 GHz band as well, e.g., the operation bandwidth of the HB element is 1.7 to 3.8 GHz [10-11]. Therefore, mitigating the interaction among cross-band antennas within a wider band is in critical demand.

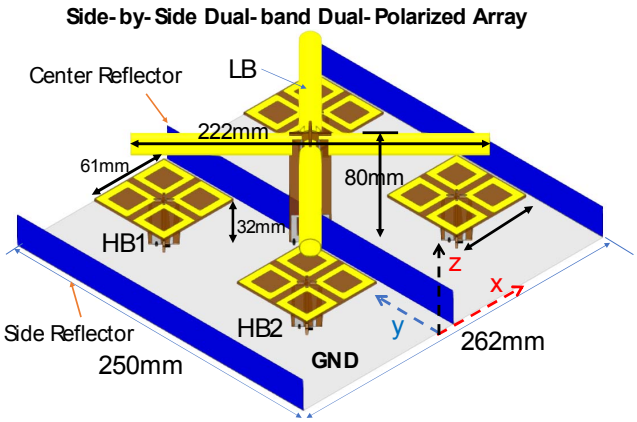

Fig. 1. A typical side-by-side dual-band dual-polarized base station antenna array section.

In this paper, we propose a different method to enhance the performance of the HB elements in a compact dual-band BSA array by optimizing the array topology. Following introduction, the cross-band interaction problem is elucidated in Section II. Section III presents two modified array topologies and illustrates their performances. In Section IV, the proposed array topology is combined with another technique, i.e., a low-scattering spiral radiator to mitigate cross-band scattering, which cured the radiation patterns and S parameters completely across the target band. Finally, the paper is concluded in Section V.

II. Problem Statement

Currently deployed 3G/4G base station antenna array usually has two columns of HB elements and one column of LB elements. The LB elements work from 698 to 960 MHz and the HB elements work from 1.7 to 2.7 GHz. Both the LB and HB elements have ±45° polarizations as a standard for base station application [12-13]. As shown in Fig. 1, this paper uses only a section of the typical side-by-side dual-band dual-polarized BSA array to conduct the study. Two columns of HB subarrays (each subarray has two HB elements) are placed side-by-side and separated by the center reflector. A LB element is located in the center of the four HB elements. In this array section, a conventional cross-dipole is used as the LB element and four tightly-coupled cross-dipoles reported in [12] are used as the HB elements.

To demonstrate how the performance of the HB element can be affected by the close proximity to the LB element, the performance of the HB antenna standing alone is presented in Fig. 2. As shown in Fig. 2(a), the reflection coefficients of the HB element for both its two polarizations are < -15 dB across the whole band. Fig. 2(b) plots the -45^0-polarized radiation patterns in the *x-z* plane at six sample frequencies. The +45°-polarized radiation patterns are similar to the -45°-polarized ones, thus are not presented for brevity. As shown in Fig. 2(b), the radiation patterns are neat and convergent.

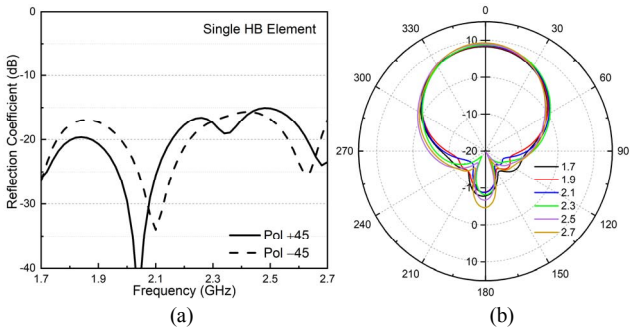

Fig. 2. (a) Reflection coefficients for the two polarizations and (b) radiation patterns for the -45°-polarization of a single HB antenna element standing alone.

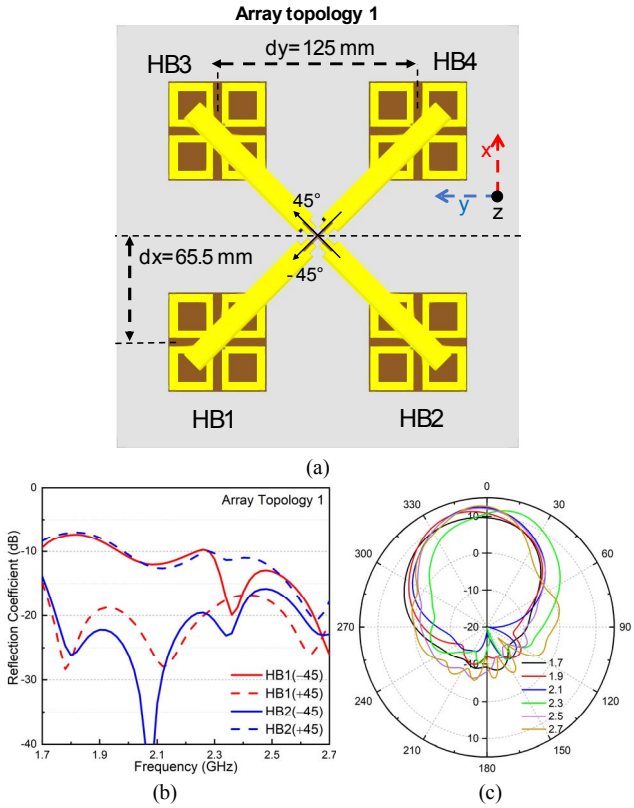

Fig. 3. (a) Top view of the array topology 1. (b) Reflection coefficients for the two polarizations of HB1 and HB2. (c) Raditiaon patterns for the -45^0 polarization of the subarray consisting of HB1 and HB2.

The HPBW is also very stable, i.e., 61° to 71°, which is critical for base station application.

However, when placing the HB element in the compact array shown in Fig. 1, the performance is degraded significantly. Fig. 3(a) gives a top-view of the array section shown in Fig. 1 and illustrates the distances between the radiators. Fig. 3(b) plots the reflection coefficients of HB1 and HB2 for both their two polarizations. It is noticed that, the impedance matching for one polarization of each HB element is ruined, i.e., the reflection coefficients are only -10

dB from 1.7 to 2.3 GHz, while they usually require to be < -15 dB in BSA. Note that for HB1, only the S parameter for the -45°-polarized radiation is deteriorated and that for the 45°-polarized port barely changes. This is because the LB arm providing the -45°-polarized radiation is place right above HB1, which leads to stronger interaction for this polarization. Similar things happen to the +45°-polarized radiation for HB2.

The radiation pattern of the HB elements has been significantly distorted as well, as demonstrated in Fig. 3(c). Note that the radiation patterns shown in Fig. 3(c) are the combined patterns of HB1 and HB2, as each HB column will work together in base station application. The beams tilt towards left and many side lobes appear. Moreover, with the frequency changing from 1.7 to 2.7 GHz, the HPBW of the HB subarray changes from 40° to 80°. The distorted radiation patterns cannot provide the required coverage, leading to signal loss in particular areas. This is generally unacceptable by cellular operators.

III. Array Topology Evolvement

The performance degradation illustrated in Figs. 3(b) and 3(c) of the HB elements is mainly due to the presence of the LB element. The LB element can be seen as a big scatterer to the HB radiation. The HB radiation can be easily captured by the LB element and reradiate. The reradiation from the LB element combines with the radiation from the HB element, resulting in the deteriorated radiation patterns at the HB. Also, the reradiation from the LB element can also excite currents on the HB elements, entering the feed port, thereby changes the impedance matching. The negative effects of the LB element on the HB elements are particularly severe under the conventional array topology (defined as array topology 1) as shown in Fig. 3(a). This is because the LB radiator locates in the near-field and is right at the boresight of the HB elements. In this section, we will show how the cross-band interactions can be mitigated by optimizing the array topology.

A. Array Topology 2

As shown in Fig. 4(a), one straightforward method to alleviate the LB element's distortion on the HB radiation is to relocate the LB element, avoiding its overlap with the HB elements in *z* direction. In array topology 2, the LB element is located in the middle of HB1 and HB3. The performances of the HB elements under this topology is illustrated in Figs. 4(b) and 4(c).

As shown in Fig. 4(b), the reflection coefficients of HB2 for both its two polarizations maintain < -15 dB. This is easy to understand because HB2 (also HB4) is further away from the LB compared to topology 1. For HB1, its reflection coefficients are also slightly improved compared to the results shown in Fig. 3(b). As for the radiation pattern, by comparing Fig. 4(b) with Fig. 3(b), it is observed that, by relocating the LB element, the main beam direction of the radiation patterns for array topology 2 is tilted back to the boresight.

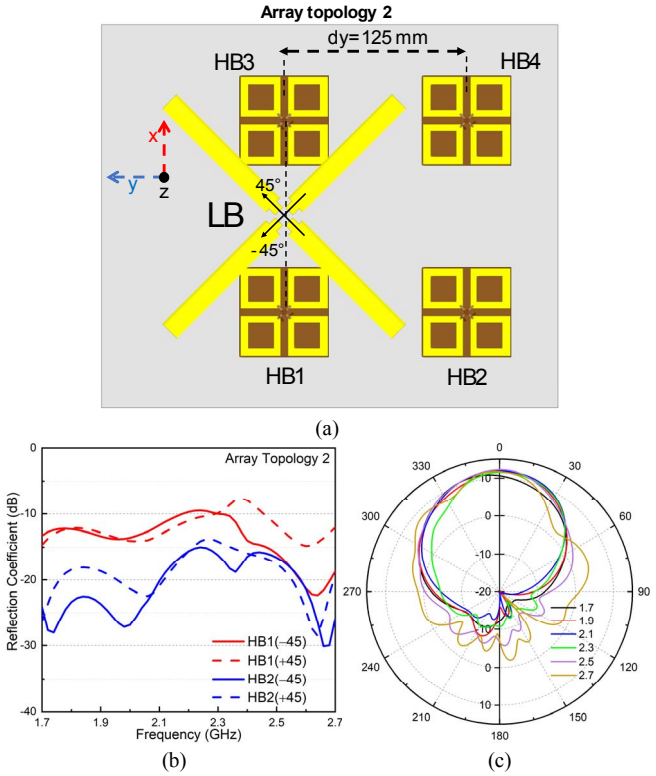

Fig. 4. (a) Top view of the array topology 2. (b) Reflection coefficients for the two polarizations of HB1 and HB2. (c) Raditiaon patterns for the -45° polarization of the subarray consisting of HB1 and HB2.

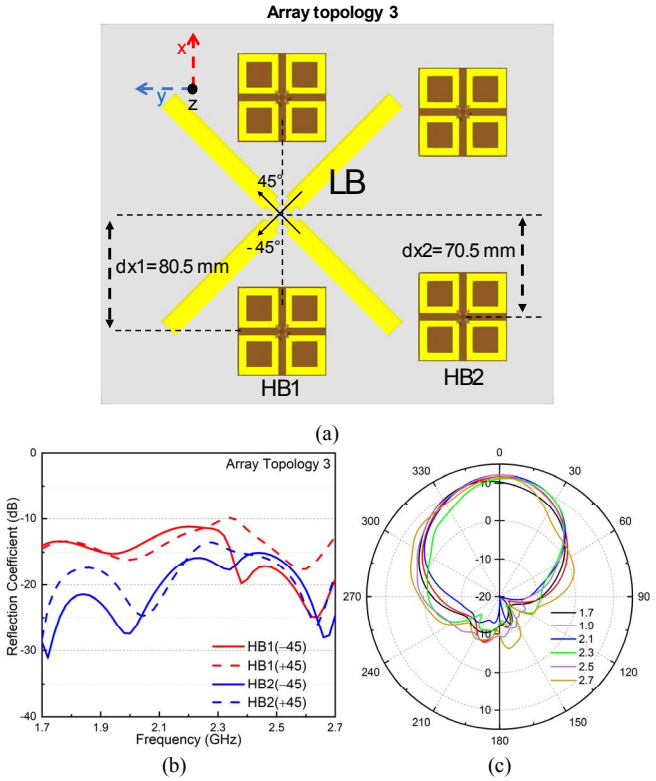

Fig. 5. (a) Top view of the array topology 3. (b) Reflection coefficients for the two polarizations of HB1 and HB2. (c) Radiation patterns for the -45° polarization of the subarray consisting of HB1 and HB2.

Noticeable performance improvement has been achieved by simply moving the LB element. However, under array topology 2, the LB element still imposes substantial negative effects on HB1 and HB3, as evidenced by the reflection coefficients. Also, the radiation patterns at higher frequencies, e.g., 2.5 and 2.7 GHz, are far from satisfaction. Besides, the HPBW variation is still severe, i.e., around 45° to 75°.

B. Array Topology 3

As mentioned above, the performance of the array topology 2 is not optimal because the LB element has a strong effect on HB1. Therefore, in array topology 3, as shown in Fig. 5(a), HB1 and HB3 are moved further apart from the LB element. The distance between HB1 and the LB element is increased from 65.5 mm to 80.5 mm. Moreover, HB2 and HB4 are also moved away from the middle for 5 mm. Note that this will not increase the width of the entire array which is mainly determined by the distance between the side reflectors. The side reflectors can be found in Fig. 1 and are hided in the top view of the array topologies for brevity.

The HB performances under array topology 3 are presented in Figs. 5(b) and 5(c). By comparing Fig. 5(b) with Fig. 4(b), it is observed that the impedance matching of HB1 is again slightly enhanced. The major improvement is on the radiation pattern by relocating the HB elements. It can be seen that the radiation patterns shown in Fig. 5(c) are much cleaner than those shown in Fig. 4(c).

IV. New Array Topology with Low-Scattering LB Element

Although previous section demonstrates that the HB performances can be substantially improved by adjusting the array topology, this method cannot solely solve the interaction issue. The reflection coefficient of HB1 shown in Fig. 5(b) under array topology 3 cannot maintain < -15 dB across the entire band. The HPBWs of the HB subarray consisting of HB1 and HB2 vary from 45° to 80°, which cannot be considered as stable.

We remark that the array topology optimization should be used with other techniques to get an optimal performance. In this work, the conventional LB dipole is replaced by the spiral dipole proposed in our previous work [7], as shown in Fig. 6(a). Such a spiral dipole has the capability to suppress the HB currents induced on it at certain frequency band, leading to a low-scattering characteristic to the HB radiation. The spiral from [7] is reoptimized to fit this scenario and its dimensions are illustrated in Fig. 6(b). Note that each spiral arm is 106 mm and the total length of the LB dipole is 222 mm, which is the same as the length of the conventional dipole shown in Figs. 3 to 5.

By placing the spiral LB element in array topology 3, the HB performances are further improved as can be seen from Figs. 6(c) and 6(d). Under array topology 4 (spiral LB + array topology 3), the reflection coefficients for both HB1 and HB2 are < -15 dB across the entire band. The radiation

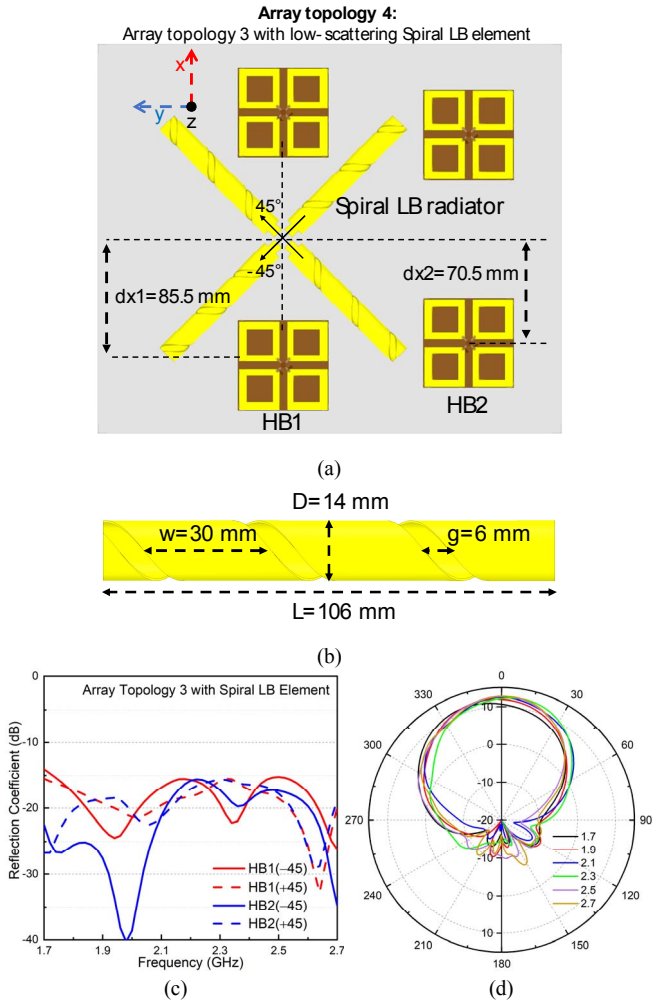

Fig. 6. (a) Top view of the array topology 3. (b) Detailed view of an arm of the spiral LB element. (c) Reflection coefficients for the two polarizations of HB1 and HB2. (d) Radiation pattern for the -45° polarization of the subarray consisting of HB1 and HB2.

patterns are also very clean and convergent. The HPBWs vary within the range of 50° to 70°.

At last, to better demonstrate how the radiation performance is improved from array topology 1 to array topology 4, the HPBWs and realized gains of the HB subarray consisting of HB1 and HB2 are compared in Figs. 7 and 8. As can be seen from Fig. 7, the array topology 4 has the smallest HPBW variation range, indicating that the radiation patterns are more stable than other topologies. Moreover, as shown in Fig. 8, the lowest gain of array topology 4 is around 11.5 dBi, which is the largest among the 4 cases.

V. Conclusion

With the continuous pursuit of antenna miniaturization, various antennas working at different bands are usually collocated on many communication platforms, e.g., in cellular base stations, to improve space efficiency. The close proximity of the antenna elements working at different bands

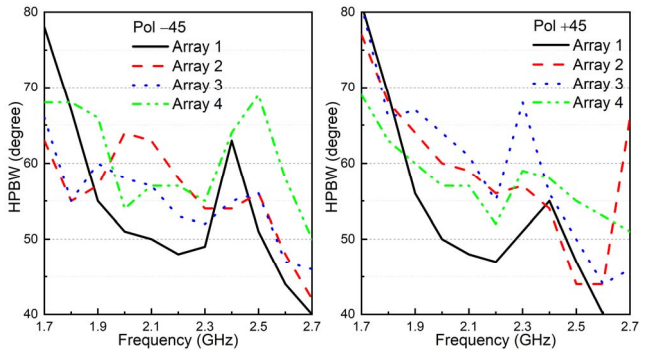

(a) (b)

Fig. 7. Comparison of the HPBW of a subarray with different array topologies for the (a) -45° polarization and (b) +45° polarization.

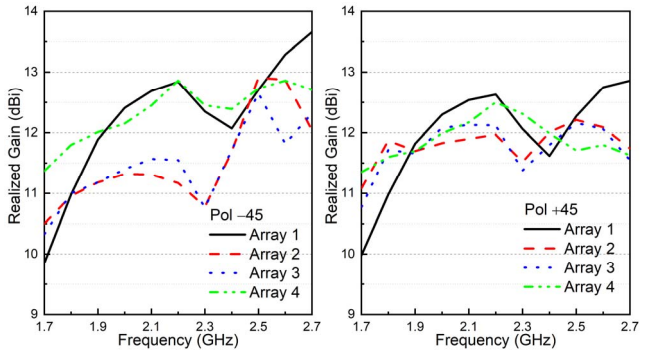

(a) (b)

Fig. 8. Comparison of the realized gain of a subarray with different array topologies for the (a) -45° polarization and (b) +45° polarization.

leads to strong, unwanted interactions, thereby significantly degrades the performance. In particular, the performance of the antennas working at higher band can be severely deteriorated by the presence of the low band antenna. This paper proposes a simple yet effective approach to mitigate such interactions by adjusting array topology. An array section of a typical dual-band dual-polarized base station antenna array is used to demonstrate the effectiveness of this method. Moreover, the optimized array topology is used with a spiral antenna having low scattering to HB radiation as LB element, leading to a compact base station antenna array with optimal performance.

ACKNOWLEDGMENT

This work was supported by the Australia Research Council (ARC) through DECRA under Grant DE200101347.

REFERENCES

[1] C. Ding, H. Sun, Y. Jay Guo and B. Jones, "Enabling the Co-Existence of Multiband Antenna Arrays," *2019 IEEE International Symposium on Phased Array System & Technology (PAST)*, Waltham, MA, USA, 2019, pp. 1-4

[2] H. Huang, Y. Liu, and S. Gong, "A dual-broadband dual-polarized base station antenna for 2G/3G/4G applications," *IEEE Antennas Wirel. Propag. Lett*., vol. 16, pp. 1111-1114, 2017.

[3] Y. He, Z. Pan, X. Cheng, Y. He, J. Qiao, M. M. Tentzeris, "A novel dual-band dual-polarized miniaturized and low-profile base station antenna", *IEEE Trans. Antennas Propag*., vol. 63, no. 12, pp. 5399-5408, Dec. 2015.

[4] Z. H. Jiang, P. E. Sieber, L. Kang, and D. H. Werner, "Restoring Intrinsic Properties of Electromagnetic Radiators Using Ultralightweight Integrated Metasurface Cloaks", *Advanced Functional Materials*, vol. 25, no. 29, pp. 4708-4716, Jun. 2015.

[5] A. Monti et al., "Mantle cloaking for co-site radio-frequency antennas," *Appl. Phys. Lett*., vol. 108, no. 11, p. 113502, 2016.

[6] A. Monti, J. Soric, A. Alù, F. Bilotti, A. Toscano, and L. Vegni, "Overcoming mutual blockage between neighboring dipole antennas using a low-profile patterned metasurface," *IEEE Antennas Wirel. Propag. Lett*., vol. 11, pp. 1414–1417, 2012.

[7] H. -H. Sun, C. Ding, H. Zhu, B. Jones, and Y. J. Guo, "Suppression of cross-band scattering in multiband antenna arrays," *IEEE Trans. Antennas Propag*., vol. 67, no. 4, pp. 2379-2389, Apr. 2019

[8] H. -H. Sun, H. Zhu, C. Ding, B. Jones and Y. J. Guo, "Scattering Suppression in a 4G and 5G Base Station Antenna Array Using Spiral Chokes," *IEEE Antennas Wirel. Propag. Lett*., vol. 19, no. 10, pp. 1818-1822, Oct. 2020

[9] X. Y. Zhang, D. Xue, L. H. Ye, Y. M. Pan, and Y. Zhang, "Compact dual-band dual-polarized interleaved two-beam array with stable radiation pattern based on filtering elements", *IEEE Trans. Antennas Propag*., vol. 65, no. 9, pp. 4566-4575, Sep. 2017.

[10] C. Ding, H. -H. Sun, H. Zhu, and Y. J. Guo, "Achieving wider bandwidth with full-wavelength dipoles (FWDs) for 5G base stations," *IEEE Trans. Antennas Propag.,* vol. 68, no. 2, pp. 1119-1127, Feb. 2020.

[11] H. -H. Sun, H. Zhu, C. Ding, and Y. J. Guo, "Dual-polarized multi-resonance antennas with broad bandwidths and compact sizes for base station applications," *IEEE Open J. Antennas Propag*., vol. 1, pp. 11-19, Dec. 2019.

[12] C. Ding, H. -H. Sun, R. W. Ziolkowski, and Y. J. Guo, "Simplified tightly-coupled cross-dipole arrangement for base station applications," *IEEE Access,* vol. 5, pp. 27491-27503, 2017.

[13] C. Ding, H. -H. Sun, Y. J. Guo, and R. W. Ziolkowski, "A dual-layered loop array antenna for base station with enhanced cross-polarization discrimination (XPD)," *IEEE Trans. Antennas Propag.,* vol. 66, no. 12, pp. 6975-6985, Sep. 2018.